Scientific
Research
Publishing

Quenching Photoluminescence of Eu(III) by Cu(II) in ZnO:Eu³⁺+Cu²⁺ Compounds by Solution Combustion Method

S. López-Romero, M. J. Quiroz Jiménez, M. García-Hipólito

Departamento de Materia Condensada y Criogenia, Instituto de Investigaciones en Materiales, Universidad Nacional Autónoma de México, Ciudad de México, México
Email: sebas@unam.mx

Abstract

In this study $Cu^{2+}+Eu^{3+}$ co-doped $ZnO(ZnO/Cu^{2+}+Eu^{3+})$ solid solution powders were synthesized by solution combustion method using as oxidant agent zinc nitrate hexahydrate and as fuel urea; the Cu^{2+} concentrations were 0, 1, 2, 3, 10, and 20 %Wt; the Eu^{3+} ion concentration was fixed in 3%Wt. The samples after were annealed at 900°C by 20 h in air. The structural results showed the largely presence of a wurtzite solid solution of $Cu^{2+}+Eu^{3+}$doped ZnO, at high Cu^{2+} doping CuO and Eu_2CuO_4 phases are also present. Morphological properties were analyzed using scanning electron microscopy (SEM) technique. However it is important to remark that the Cu^{2+} ions suppress the Eu^{3+} ion photoluminescence (PL) by means of an overlap mechanism between Cu^{2+} absorption band and Eu^{3+}emission band (e.g. $^5D_0 \rightarrow {}^7F_2$) of the Eu^{3+} emission spectra.

Keywords

ZnO, Co-Doped $Cu^{2+}+Eu^{3+}$, Quenching, Photoluminescence, Solution, Combustion

1. Introduction

Zinc oxide (ZnO) is actually considered to be a II-VI semiconductor material of great importance in basic science as in technologic applications due to its important properties physical and chemicals: the ZnO has a band gap energy of 3.7 eV [1]-[6], an large exciton bonding energy of 60 meV, also has defects as O and Zn vacancies; however it is chemically and thermally stable and friendly with the environment. Due to these properties, the ZnO can be utilized in the fabrication of devices such as: electro-optical devices [7], gas sensors [8], catalyst [9], piezoelectric device [10], electro-optical [11], photovoltaic [12], paramagnetic [13], etc. Several methods for

the production of ZnO undoped and doped with various types of dopants (rare heart, metals, lanthanides, etc.) [14]-[17] have been described, such as, electrodeposition [18], evaporation [19], vapor-liquid-solid (VLS) growth [20], metal organic catalyst assisted vapor-phase epitaxy [21], aqueous thermal decomposition [22], microwave activated chemical bath deposition (MW-CBD) [23], chemical bath deposition (CBD) [24], surfactant-assisted hydrothermal method [25], solution combustion [26] etc. This last method is more convenient than other because it is very fast, and less expensive; it has an easier composition control, and coating can be deposited on large area etc. The introduction of Cu^{2+} ions into ZnO lattice sums or produces changes that improve the ZnO properties such as: band gap tailored, magnetic and electrical properties, passivation of defects, as p-type dopant in the original n-type ZnO semiconductor. However, actually it is well known that the co-doping with Cu^{2+} ion in Eu^{3+} doped glasses photoluminescent compounds the Cu^{2+} ion can quench the Eu^{3+} photoluminescence [27]-[29] with the increase of the Cu^{2+} ion concentration in glasses matrix; this quenching effect can be used to tuning between ultra-violet and visible emission in devise photoluminescent. In this study co-doped $ZnO/Cu^{2+} + Eu^{3+}$ solid solution powders have been synthesized by solution combustion method as a function of the Cu^{2+} ion concentration in %Wt. maintaining the Eu^{3+} ion concentration constant at a value of 3% Wt. Finally the sample was annealed at 900˚C by 20 h. Also it is demonstrated that the quenching Eu^{3+} PL by the copper ion action also occurs in ZnO matrix.

2. Experimental

The synthesis method solution combustion is simple and fast caused by the chemical reaction oxidation-reduction (REDOX) highly exothermic (1200˚C) [18] between an oxidizer agent and an fuel, in this experiment Zinc nitrate hexahydrate $(Zn(NO_3)_2 \cdot 6H_2)$ was used as oxidizer agent and urea (NH_2CONH_2) as fuel, copper chloride $(CuCl_2)$ and Europium chloride $(EuCl_3)$ were used as dopants agents. The next chemical reaction (REDOX) between the oxidizer agent and the fuel is an reaction highly exothermic and is the Stoichiometric reaction obtained with a equivalence ratio value of unity (*i.e.* f = O/F = 1) where O and F are the total oxidizing and total reduction valences of the components and the energy released by the combustion is at maximum [18]. With this reaction are obtained the follow products: ZnO, H_2O (vapor), CO_2, and N_2.

$$3Zn\left(NO_3\right)_2 \cdot 6H_2O + 5H_2NCONH_2 \rightarrow 3ZnO + 16H_2O + 5CO_2 + 8N_2 + heat \tag{1}$$
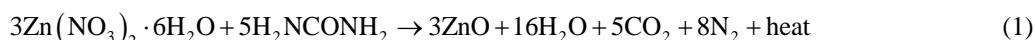
Using the atomic weight concept, the Equation (1) was translated to grams/mol and used to obtain 3 gr of ZnO powder. The Cu^{2+} ion dopant concentration values were 0, 1, 2, 3, 10, and 20 wt%. The Eu^{3+} ion dopant concentration was maintained constant at 3 Wt% with respect to 3 gr of ZnO. From the translated grams/mol Equation (1) (no shown), 8.31 gr of $Zn(NO_3)_2 \cdot 6H_2O$, 3.68 gr of H_2NCONH_2 plus the numerous of grams corresponding to each Cu^{2+} ion concentration plus 3 Wt% Eu^{3+} ion were mixing with 20 ml of H_2O and stirring vigorously in a flask glass and after put on a hot plate at 500˚C, after of few minutes the reactive solution boils, foams, ignites, and burns with an incandescent flame at an approximate temperature of 1200˚C [18] producing 3 gr of ZnO powders approximately. After all the samples are annealing at 900˚C by 24 h. The $ZnO/Cu^{2+}+Eu^{3+}$ samples thus obtained were structurally characterized by X-ray diffraction (XRD) technique using a Philips PW 1800 diffractometer with Cu kα radiation (1.5406 Å), the photoluminescence (PL) of the $ZnO/Cu^{2+}+Eu^{3+}$ samples was studied by means of a spectrofluorometer Fluoro Max-P that uses a xenon lampas excitation source, The wavelength excitation was of 270 nm, and finally, the morphology of the $ZnO/Cu^{2+}+Eu^{3+}$ powders was recorded using a scanning electron microscopy (SEM) JEOL JSM 840 A.

3. Results and Discussion

3.1. Structural Characterization

The **Figure 1** shows the X-ray diffractograms of the $ZnO/Cu^{2+}+Eu^{3+}$ powders as a function of the Cu^{2+} ion concentration and annealing at 900˚C by 20 h. From the XRD patterns, can be observed that for the Cu^{2+} doping of 1, 2, 3, 10 and 20%Wt all the diffraction peaks can be indexed to the majority phase hexagonal wurtzite type ZnO structure for all samples (JCPDS card #89-(102)), also, for the Cu^{2+} ion concentrations of 1, 2, 3 and 10%Wt a peak at $2\theta = 28.5°$ is present and is assigned to the minority Eu_2O_3 phase (JPDAS card #86-2476). The diffractograms also reveal the high crystallinity of the product for the five Cu^{2+} ion concentrations, for the higher Cu^{2+} concentrations of 10 and 20%Wt. A peak corresponding to the Eu_2CuO_4 molecules is present; effectively:

in **Figure 2** can be see the peak at the 2theta scale at 24° correspond to the Eu_2CuO_4 phase, however also in **Figure 2** appear all the peaks characteristic of the zinc oxide majority phase reported in this text.

Comparatively, contrary to the observation of Iribarren *et al.* [17] obtained from your experiments on Cu^{2+} doped ZnO, in our diffractograms can be not observed a little shift initially toward higher angles of the principal peak (101) until 3%Wt of Cu^{2+} where an maximum is reached, after at higher Cu^{2+} concentrations the angular displacement is toward lower angles, in the first case this is due to the substitution of the Zn ion with 0.06 nm size by the smaller Cu^{2+} ion with 0.057 nm size that cause an lattice parameter shrinkage, in the second case this is attributed to an relative saturation of the Cu^{2+} ions on the samples surface, in our case the not presence of angular changes can be due to the Eu^{3+} ions present in the ZnO lattice. No diffraction peaks were detected from other impurities. Using the Scherrer formula, the average crystallite size calculated from characteristic peak (101) was 160 nm for the ZnO intrinsic and decreased to 150 nm for the $ZnO/Cu^{2+}+Eu^{3+}$ samples doped with 10 Wt% of Cu^{2+} ion concentration.
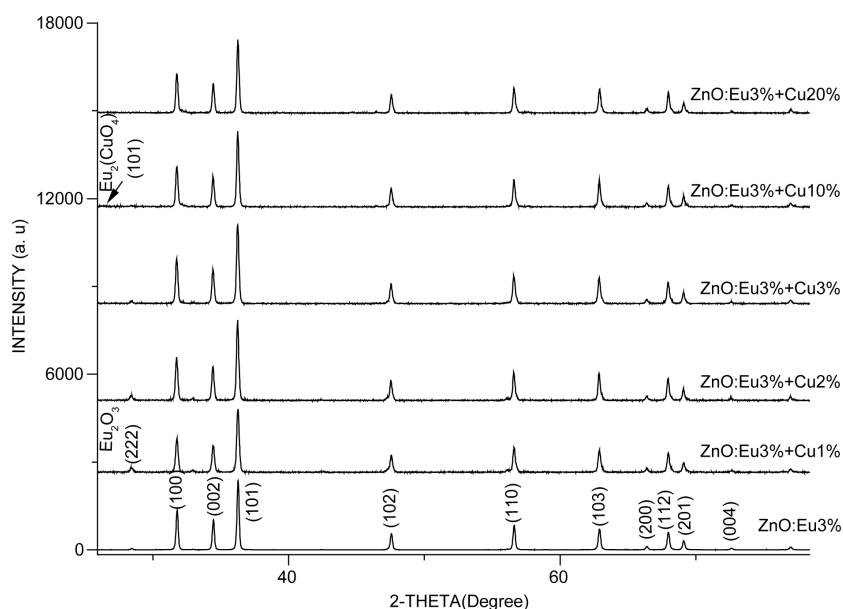

Figure 1. XRD spectra of the $Cu^{2+}+Eu^{3+}$ doped ZnO as a function of the Cu^{2+} ion concentration in %Wt.
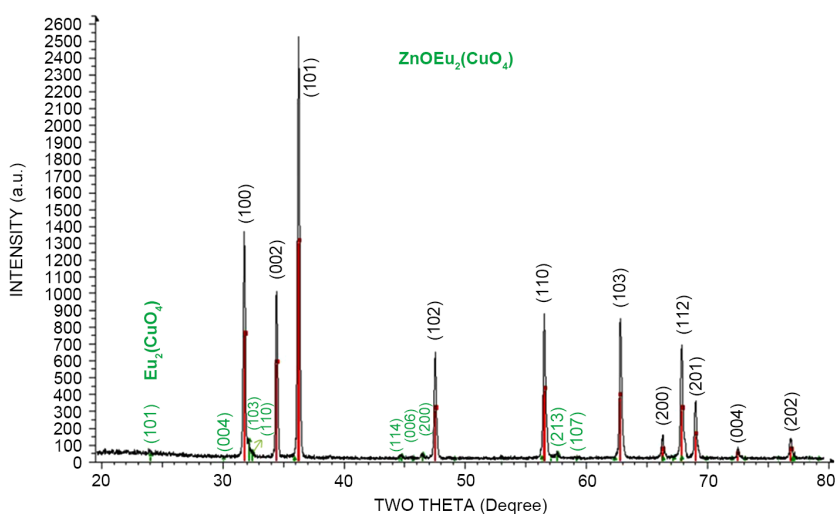

Figure 2. XRD diffractogram of the ZnO and Eu_2CuO_4 compound. Cu^{2+} ion concentration for this figure was of 20 wt%.

3.2. Morphological Study

The **Figure 3(a)** shows the SEM image of the form of the Eu^{3+} doped ZnO whit out Cu^{2+} ions, it is observed that the Eu^{3+}/ZnO crystallites are agglomerated forming amorphous particles of 1.5 µm of large in an approximation. The **Figure 3(b)** shows the SEM image of a particle of $Cu^{2+}+Eu^{3+}$ doped ZnO polycrystalline particles, it can be see that the individual crystallites are agglomerated forming amorphous particles whit 2 µm side and 3 µm of large approximated.
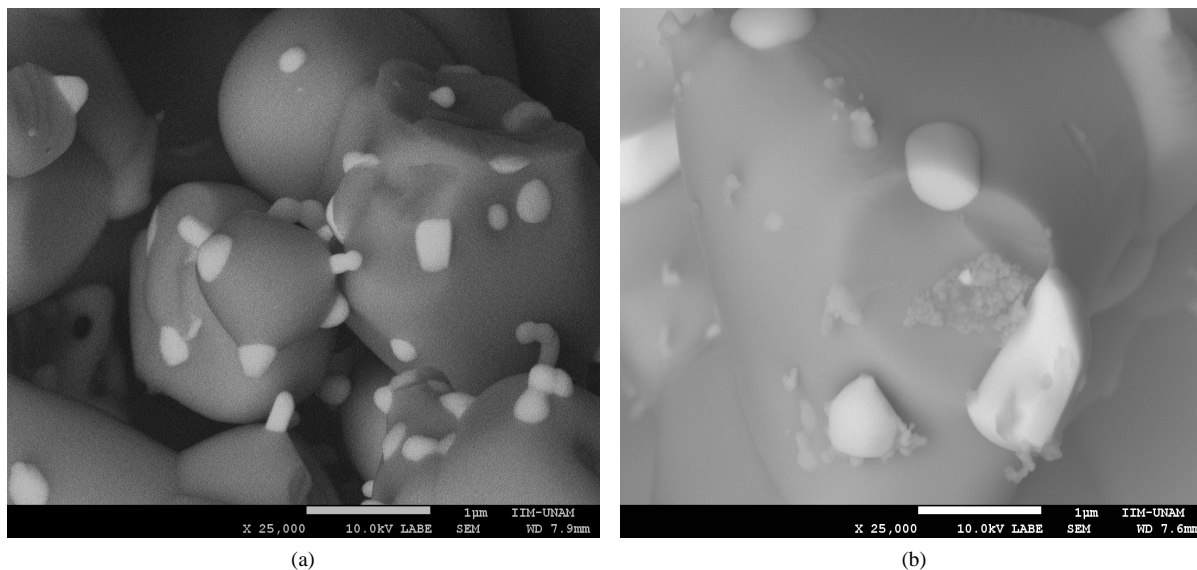

(a)   (b)

Figure 3. SEM images of (a) undoped ZnO and (b) $Cu^{2+}+Eu^{3+}$ doped ZnO with 10%Wt Cu ions.

3.3. Photoluminescence Study

The **Figure 4(a)** and **Figure 4(b)** shows the room temperature photoluminescence spectra (PL) of the Eu^{3+} doped ZnO without the Cu^{2+} ion dopant and of the $Cu^{2+}+Eu^{3+}$ doped ZnO (ZnO:$Cu^{2+}+Eu^{3+}$) nanocrystals as a function of the Cu^{2+} ion concentration in Wt% and after both samples undoped and doped with the Cu^{2+} were annealing at 900°C by 24 h, the samples were irradiated with an excitation wavelength of 270 nm (in the UV range). In **Figure 4(a)** it is observed that the PL spectra correspond to the Eu^{3+} ion emission in a ZnO matrix, in particular the most intense peak at the visible color red whit 613 nm in wavelength [27]. However it is observed from **Figure 4(b)** that the ZnO:$Cu^{2+}+Eu^{3+}$ samples doped with 1, 2, 3, 10, and 20 Wt% are all alike: because they does not present antypical green broad emission band from 400 nm to 600 nm centered about 516 nm [28] as is showed in **Figure 4(a)**, this band is due to the intrinsic defects emission of ZnO host. However, in the PL spectra of the ZnO:$Cu^{2+}+Eu^{3+}$ samples two peaks at the UV region in 350 and 380 nm are present, in this the intensity of this last peak I this observer that your intensity it is decreased at an concentration of 20% Cu^{2+}, this decrease is due to the capacity of Quenching of the Cu^{2+} at hide concentration the first peak is attributed to the 5d→7f europium transition, the second band is attributed to near edge band (NEB) emission [29], other peak at the violet-blue region centered about 420 nm also is observed, this peak is due to the 5D→4F Eu^{3+} transition. From the photoluminescence spectra corresponding to the Eu^{3+} ion also appear: the peaks at 591, 613 and 630 nm are related to the direct intra-4f transitions in Eu^{3+} ions $^5D_0 \rightarrow {}^7F_j$ (j = 1, 2, 3), the most intense emission is associated to the $^5D_0 \rightarrow {}^7F_2$ transition in the red spectral region (613 nm) and is due to a allowed electric-dipole transition with inversion antisymmetric [28] [30], which results in a large transition probability in the crystal field [31]-[34]. The peak at 591 nm is due to the $^5D_0 \rightarrow {}^7F_1$ transition, is an allowed magnetic-dipole transition. The peak at 579 nm is due to the forbidden $^5D_0 \rightarrow {}^7F_0$ transition due to the same total angular momentum, indicating that some Eu^{3+} ions possibly occupy other sites as interstitial sites [35]-[38]. It is very important to note from the photoluminescence spectra that as increase the Cu^{2+} ion concentration in the ZnO:$Cu^{2+}+Eu^{3+}$ samples the intensity of the most intense transition of the Eu^{3+} ion with red wavelength of 613 nm decrease until an negligible value while the intensity of the wavelength emission at 380 nm situated in the UV region increase until

reach an constant value for high Cu^{2+} ion concentrations: effectively: the **Figure 5** shows the emission intensity variation of the red $^5D_0 \rightarrow {}^7F_2$ transition of the Eu^{3+} ion and of the UV emission peak at 380 nm of the $ZnO:Cu^{2+}+$ Eu^{3+} samples as a function of the Cu^{2+} ion concentration, the graphic shows that as the Cu^{2+} ion concentration increase the red color intensity decrease until an minimum value while the intensity of the UV emission increase until obtain an constant value. It has been reported that divalent copper ion can effectively suppress Eu^{3+} photo-luminescence, in an matrix of glass this is due to the quenching effect of Cu^{2+}impuritieson Eu^{3+} emission photo-luminescence quenching resulting from $Eu^{3+} \rightarrow Cu^{2+}$ non-radiative energy transfer in which an spectral overlap occurring between Cu^{2+} absorption and Eu^{3+} emission(e.g. $^5D_0 \rightarrow {}^7F_2$) transition occur [28] [29]. Thus, in this paper is postulated that the quenching of the Eu^{3+} photoluminescence also can occur in ZnO matrix.
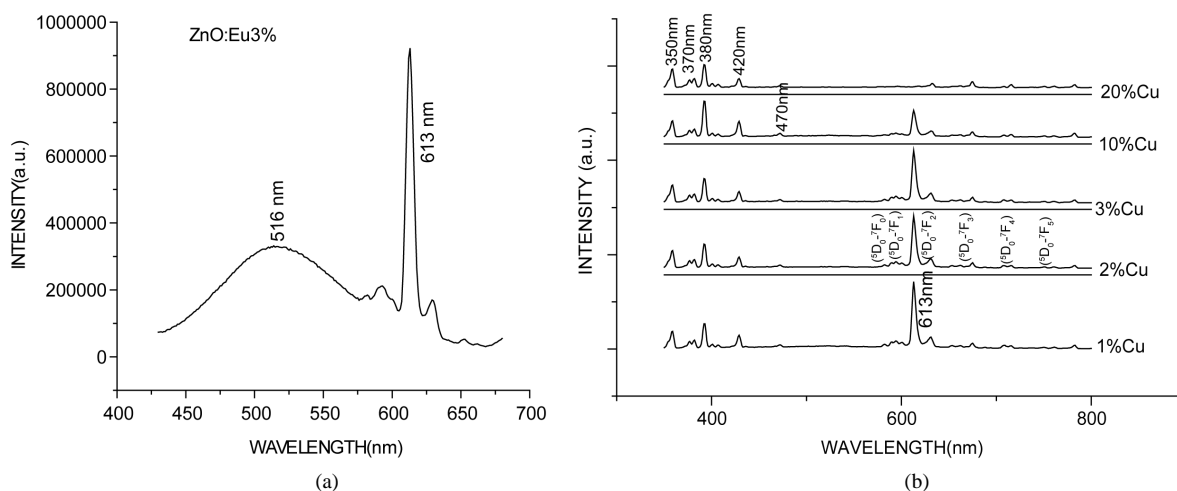

Figure 4. (a) Photoluminescence spectra of Eu^{3+} doped ZnO at 3%Wt; (b) Photoluminescence spectra of $Cu^{2+}+Eu^{3+}$ doped ZnO as a function of the Cu^{2+} ion concentration in %Wt.
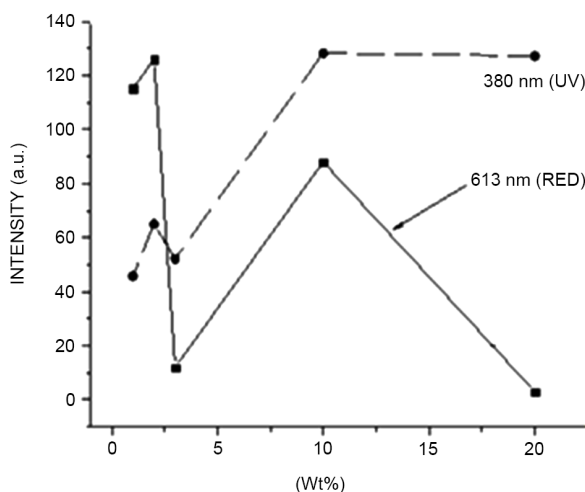

Figure 5. Intensity of the emissions Wavelength 380 and 613 nm as a function of the Cu^{2+} ion concentration in %Wt.

4. Conclusion

In this study $Cu^{2+}+Eu^{3+}$ doped ZnO solid solution powders were synthesized by solution combustion method maintaining the Eu^{3+} ion concentration fixed at 3%Wt and after annealing at 900°C by 24 h. From the XRD study it is confirmed that the ZnO hexagonal wurtzite structure is conserved after the introduction of the Cu^{2+} ion in the ZnO structure, and the same XRD study showed the presence of the minority phases Eu_2O_3 and Eu_2CuO_4. From photoluminescence study it is demonstrated that the Cu^{2+} ion effectively suppresses the Eu^{3+} ion

photoluminescence due to the PL quenching effect of the Cu^{2+} ion on the Eu^{3+} ion.

Acknowledgements

References

[1] Iribarren, A., Fernandez, P. and Piqueiras, I. (2008) Catodoluminescence of ZnO:Te with ZnTe and TeO_2 Doping Precursors. *Superlattices and Microstructures*, **43**, 600-604. http://dx.doi.org/10.1016/j.spmi.2007.06.009

[2] Rahmani, M.B., Keshmiri, S.H., Shafiei, M., Latham, K., Wlodarski, W., Plessis, J.D. and Kalantar-Zadeh, K. (2009) Transition from *n*- to *p*-Type of Spray Pyrolysis Deposited Cu Doped ZnO Thin Films for NO_2 Sensing. *Sensor Letters*, **7**, 1-8. http://dx.doi.org/10.1166/sl.2009.1121

[3] Lee, J.-B., Lee, H.-J., Seo, S.-H. and Park, J.-S. (2001) Characterization of Undoped and Cu-Doped ZnO Films for Surface Acoustic Wave Applications. *Thin Solid Films*, **398-399**, 641-646. http://dx.doi.org/10.1016/S0040-6090(01)01332-3

[4] Gao, D.Q., Xue,. D.S., Xu, Y., Yan, Z.J. and Zhang, Z.H. (2009) Synthesis and Magnetic Properties of Cu-Doped ZnO Nanowire Arrays. *Electrochimica Acta*, **54**, 2392-2395. http://dx.doi.org/10.1016/j.electacta.2008.10.051

[5] Qi, J., Gao, D.Q., Zhang, L. and Yang, Y.H. (2010) Room-Temperature Ferromagnetism of the Amorphous Cu-Doped ZnO Thin Films. *Applied Surface Science*, **256**, 2507-2508. http://dx.doi.org/10.1016/j.apsusc.2009.10.096

[6] Lupan, O., Pauporté, T., Viana, B. and Aschehoug, P. (2011) Electrodeposition of Cu-Doped ZnO Nanowire Arrays and Heterojunction Formation with *p*-GaN for Color Tunable Light Emitting Diode Applications. *Electrochimica Acta*, **56**, 10543-10549. http://dx.doi.org/10.1016/j.electacta.2011.02.004

[7] Pauporté, Th. and Lincot, D. (1999) Heteroepitaxial Electrodeposition of Zinc Oxide Films on Gallium Nitride. *Applied Physics Letters*, **75**, 3817-3891. http://dx.doi.org/10.1063/1.125466

[8] Mikami, M., Eto, T., Wang, J.F., Masa, Y. and Isshiki, M. (2007) Growth of Zinc Oxide by Chemical Vapor Transport *Journal of Crystal Growth*, **304**, 37-41.

[9] Levitt, A.P. (1970) Whisquer Technology. Wiley-Interscience, New York.

[10] Park, W.I., Kim, D.H., Jung, S.-W. and Yi, G.-C. (2002) Metalorganic Vapor-Phase Epitaxial Growth of Vertically Well-Aligned ZnO Nanorods. *Applied Physics Letters*, **80**, 4232-4234. http://dx.doi.org/10.1063/1.1482800

[11] Vayssieres, L., Keis, K., Lindquist, S.-E. and Hagfeldt, A. (2001) Purpose-Built Anisotropic Metal Oxide Material: 3D Highly Oriented Microrod Array of ZnO. *The Journal of Physical Chemistry B*, **105**, 3350-3352. http://dx.doi.org/10.1021/jp010026s

[12] Wang, W.-W. and Zhu, Y.-J. (2004)Shape-Controlled Synthesis of Zinc Oxide by Microwave Heating Using an Imidazolium Salt. *Inorganic Chemical Communications*, **7**, 1003-1005. http://dx.doi.org/10.1016/j.inoche.2004.06.014

[13] Zwingel, D. and Gärtner, F. (1974) Paramagnetic and Optical Properties of Na-Doped ZnO Single Crystals. *Solid State Communications*, **14**, 45-49.

[14] Sridevi, D. and Rajendran, K.V. (2010) Enhanced Optical Properties La Doped ZnO Nanoparticles Department of Physics, Presidency College, Chennai-5, India. *Optoelectronics and Advanced Materials—Rapid Communications*, **4**, 1591-1593

[15] Molahasani, N., Sadjadi, M.S. and Zare, K. (2013) Correlation of Morphology and Luminescent Properties of ZnO Nano Particles to Different Surfactants via Hydrothermal Method. *International Journal of Nano Dimension*, **4**, 161-166.

[16] Zhang, J., Liu, H., Wang, Z., Ming, N., Li, Z. and Biris, A.S. (2007) Polyvinylpyrrolidone-Directed Crystallization of ZnO with Tunable Morphology and Bandgap. *Advanced Functional Materials*, **17**, 3897-3905. http://dx.doi.org/10.1002/adfm.200700734

[17] Iribarren, A., Hernández-Rodríguez, E. and Maqueira, L. (2014) Structural, Chemical and Optical Evaluation of Cu-Doped ZnO Nanoparticles Synthesized by an Aqueous Solution Method. *Materials Research Bulletin*, **60**, 376-381.

[18] Miamani, T. and Patil, K.C. (2001) Solution Combustion Synthesis of Nanoscale Oxides and Their Composites. *Materials Physics and Mechanics*, **4**, 134-137.

[19] Chow, L., Lupan, O., Chai, G., Khallaf, H., Ono, L.K., Roldan Cuenya, B., Tiginyanu, I.M., Ursaki, V.V., Sontea, V. and Schultea, A. (2013) Synthesis and Characterization of Cu-Doped ZnO One-Dimensional Structures for Miniaturized Sensor Applications with Faster Response. *Sensors and Actuators A*: *Physical*, **189**, 399-408.

http://dx.doi.org/10.1016/j.sna.2012.09.006

[20] Xing, G.Z., Yi, J.B., Tao, J.G., Liu, T., Wong, L.M., Zhang, Z., Li, G.P., Wang, S.J., Ding, J., Sum, T.C., Huan, C.H.A. and Wu, T. (2008) Comparative Study of Room-Temperature Ferromagnetism in Cu-Doped ZnO Nanowires Enhanced by Structural Inhomogeneity. *Advanced Materials*, **20**, 3521-3527. http://dx.doi.org/10.1002/adma.200703149

[21] Singhal, S., Kaur, J., Namgyal, T. and Sharma, R. (2012) Cu-Doped ZnO Nanoparticles: Synthesis, Structural and Electrical Properties. *Physica B*: *Condensed Matter*, **407**, 1223-1226. http://dx.doi.org/10.1016/j.physb.2012.01.103

[22] Öztas, M. and Bedir, M. (2008) Thickness Dependence of Structural, Electrical and Optical Properties of Sprayed ZnO:Cu Films. *Thin Solid Films*, **516**, 1703-1709. http://dx.doi.org/10.1016/j.tsf.2007.05.018

[23] Bellini, J.V., Morelli, M.R. and Kiminami, R.H.G.A. (2002) Electrical Properties of Polycrystalline ZnO:Cu Obtained from Freeze-Dried ZnO+Copper(II) Acetate Powders. *Journal of Materials Science*: *Materials in Electronics*, **13**, 485-489. http://dx.doi.org/10.1023/A:1016160204435

[24] Liu, Y., Liang, H.W., Xu, L., Zhao, J.Z., Bian, J.M., Luo, Y.M., Liu, Y., Li, W.C., Wu, G.G. and Du, G.T. (2010) Cu Related Doublets Green Band Emission in ZnO:Cu Thin Films. *Journal of Applied Physics*, **108**, 113507. http://dx.doi.org/10.1063/1.3516459

[25] Tian, Y.F., Li, Y.F., He, M., Putra, I.A., Peng, H.Y., Yao, B., Cheong, S.A. and Wu, T. (2011) Bound Magnetic Polarons and *p-d* Exchange Interaction in Ferromagnetic Insulating Cu-Doped ZnO. *Applied Physics Letters*, **98**, 162503. http://dx.doi.org/10.1063/1.3579544

[26] Reddy, A.J., Kokila, M.K., Nagabhushana, H., Chakradhar, R.P.S., Shivakumara, C., Rao, J.L. and Nagabhushana, B.M. (2011) Structural, Optical and EPR Studies on ZnO:Cu Nanopowders Prepared via Low Temperature Solution Combustion Synthesis. *Journal of Alloys and Compounds*, **509**, 5349-5355. http://dx.doi.org/10.1016/j.jallcom.2011.02.043

[27] López-Romero, S., Quiroz-Jiménez, M.J., García, M.H. and Aguilar-Castillo, A. (2014) Bright Red Luminescence and Structural Properties of Eu^{3+} Ion Doped ZnO by Solution Combustion Technique. *World Journal of Condensed Matter Physics*, **4**, 227-234.

[28] Jiménez, J.A. (2015) Photoluminescence of Eu^{3+}-Doped Glasses with Cu^{2+} Impurities. *Spectrochimica Acta Part A*: *Molecular and Biomolecular Spectroscopy*, **145**, 482-486. http://dx.doi.org/10.1016/j.saa.2015.03.047

[29] Batyaev, I.M. and Tinus, A.M. (1998) Transport of Electronic Excitation Energy in Solid-State Glassy Phosphors Activated with Europium (III) and Copper (II). A.I. Gerstsen Russian State Pedagogical University, St. Petersburg. *Pis'ma Zh. Tekh. Fiz*, **24**, 59-61.

[30] Sharma, P.K., Dutta, R.K. and Pandey, A.C. (2009) Doping Dependent Room-Temperature Ferromagnetism and Structural Properties of Dilute Magnetic Semiconductor ZnO:Cu^{2+} Nanorods. *Journal of Magnetism and Magnetic*, **321**, 4001-4005. http://dx.doi.org/10.1016/j.jmmm.2009.07.066

[31] Ursaki, V., Rusu, E., Zalamai, V., *et al*. (2004) Photoluminescence of Eu Doped ZnO Structures. *Proceeding of SPIE* 5822, Chisinau, 3 May 2004, 148.

[32] Fujihara, S.O., Suzuqui, A. and Kimura, T. (2003) Ga-Doping Effects on Electrical and Luminescent Properties of ZnO: (La,Eu) of Red Phosphor Thin Films. *Journal of Applied Physics*, **94**, 2411-2416. http://dx.doi.org/10.1063/1.1594817

[33] Qi, J.F., Matsumoto, T., Tanaka, M. and Masumoto, Y. (2000) Europium Silicate Thin Films on Si Substrates Fabricates by a Radio Frequency Sputtering Method. *Journal of Physics D*: *Applied Physics*, **33**, 2074. http://dx.doi.org/10.1088/0022-3727/33/16/321

[34] Ningthoujam, R.S. and Nanoci, J. (2008) Dispersible Li+ and Eu^{3+} Co-Doped Nanocrystalline: ZnO Luminescence and EPR Studies. *Journal of Nanoscience and Nanotechnology*, **8**, 3059-3062. http://dx.doi.org/10.1166/jnn.2008.152

[35] Chen, P.L., Ma, X.Y. and Yang, D.R. (2007) ZnO:Eu Thin Films: Sol-Gel Derivation and Strong Photoluminescence from $^5D_0 \rightarrow {}^7F_0$ Transition of Eu^{3+} Ions. *Journal of Alloys and Compounds*, **431**, 317-320. http://dx.doi.org/10.1016/j.jallcom.2006.05.078

[36] Luo, L., Gong, L., Liu, Y.F., *et al*. (2010) Enhanced Ultraviolet Lasing from Europium-Doped Zinc Oxide Nanocrystals. *Optical Materials*, **32**, 1066-1070. http://dx.doi.org/10.1016/j.optmat.2010.02.032

[37] Hsu, C.-H., Chen, L.-C. and Zhang, X.Y. (2014) Effect of the Cu Source on Optical Properties of CuZnO Films Deposited by Ultrasonic Spraying. *Materials*, **7**, 1261-1270.

[38] Babikier, M., Wang, D.B., Wang, J.Z., Li, Q., Sun, J.M., Yan, Y., Yu, Q.J. and Jiao, S.J. (2014) Cu-Doped ZnO Nanorod Arrays: The Effects of Copper Precursor and Concentration. *Nanoscale Research Letters*, **9**, 199. http://dx.doi.org/10.1186/1556-276X-9-199

Scientific Research Publishing

Submit or recommend next manuscript to SCIRP and we will provide best service for you:

Accepting pre-submission inquiries through Email, Facebook, LinkedIn, Twitter, etc.

A wide selection of journals (inclusive of 9 subjects, more than 200 journals)

Providing 24-hour high-quality service

User-friendly online submission system

Fair and swift peer-review system

Efficient typesetting and proofreading procedure

Display of the result of downloads and visits, as well as the number of cited articles

Maximum dissemination of your research work

Submit your manuscript at: http://papersubmission.scirp.org/